Rapid #: -21072770

CROSS REF ID: **321991**

LENDER: **OUU (OU-Tulsa) :: Schusterman Library**

BORROWER: **UMR (Missouri University of Science and Technology) :: Main Library**

TYPE:	Article CC:CCG
JOURNAL TITLE:	Journal of molecular spectroscopy
USER JOURNAL TITLE:	Journal of Molecular Spectroscopy
ARTICLE TITLE:	Broadband microwave spectroscopy of cyclopentylsilane and 1,1,1-trifluorocyclopentylsilane
ARTICLE AUTHOR:	Licaj, Lucas,
VOLUME:	390
ISSUE:	
MONTH:	
YEAR:	2022
PAGES:	111698-
ISSN:	0022-2852
OCLC #:	

Processed by RapidX: 7/31/2023 11:41:34 AM

Journal of Molecular Spectroscopy 390 (2022) 111698

Contents lists available at ScienceDirect

Journal of Molecular Spectroscopy

journal homepage: www.elsevier.com/locate/yjmsp

Broadband microwave spectroscopy of cyclopentylsilane and 1,1,1-trifluorocyclopentylsilane

Lucas Licaj [a], Nicole Moon [b], Garry S. Grubbs II [b], Gamil A. Guirgis [a,*], Nathan A. Seifert [c,*]

[a] Department of Chemistry and Biochemistry, College of Charleston, Charleston, SC 29424, United States
[b] Department of Chemistry, Missouri University of Science and Technology, Rolla, MO 65409, United States
[c] Department of Chemistry and Chemical & Biomedical Engineering, University of New Haven, West Haven, CT 06516, United States

ARTICLE INFO

Additional dedication: Prof. James Patton Deavor.

Keywords:
Microwave spectroscopy
Structure determination
Organosilicon compounds
Large amplitude motion

ABSTRACT

The broadband microwave spectra of two related organosilicon molecules, cyclopentylsilane and 1,1,1-trifluorocyclopentylsilane, have been measured and assigned. Both molecules exhibit a C_s-symmetric "envelope" structure, which is confirmed by a determination of the heavy atom backbone r_s substitution structures using isotopic substitution in natural abundance, as well as the presence of strong *a*-type transitions, weaker *c*-type, and a non-detection of *b*-type transitions, indicative of a mirror plane perpendicular to the prolate symmetry axis of the molecule. Both molecules appear to have significant zero-point vibrational averaging of their ring twisting and puckering coordinates, which lead to deviations between the ground state experimental structure and the predicted equilibrium structures at the B3LYP-D3/def2-TZVP level of theory. Additionally, we observe an excited vibrational state associated with this large amplitude motion and we use a simple perturbation theory argument to confirm the identity of these excited state carriers.

1. Introduction

In the high resolution spectroscopy of flexible organic molecules, large amplitude motions as sources of perturbations to spectra and their resultant influence on experimental methods for structure determination have been studied in a wide variety of systems, from the internal rotation splittings of methylated species [1], Coriolis-mediated coupling in *gauche-gauche* tunneling in alcohols [2], and the puckering of small ring structures [3–5]. However, zero-point averaging across the shallow, anharmonic potential energy surfaces of some large amplitude motions can affect the spectroscopy of affected molecules in subtler ways than formal perturbations of the spectra. For instance, low frequency modes can appreciably affect the ground state averaged structure of a molecule such that standard methods for determining structure from spectra, such as through Kraitchman's equations, can lead to non-physical results.

Here, we approach the issue of vibrational averaging in small ring systems through the addition of silane substitutent groups to a cyclopentane frame. In particular, we present the broadband rotational spectroscopy of cyclopentylsilane (abbreviated here as CPS), the silicon analogue of methylcyclopentane, and its trifluorinated sibling, 1,1,1-trifluorocyclopentylsilane (abbreviated TFCPS). This is the first spectroscopic measurement of the trifluorinated analogue known to the authors. However, CPS has been studied in the past using lower resolution spectroscopic methods, such as through Raman and IR spectroscopy by Durig and coworkers [6], and gas-phase electron diffraction by Shen & Dakkouri [7]. Also, the electronic effects of a silicon substitutent on 5-member hydrocarbon rings has also been explored in detail theoretically [8].

Both studies show results that suggest that the cyclopentane ring exhibits large amplitude motion through a ring twisting potential that exchanges the structure between its equatorial and axial conformations [9]. While the electron diffraction study suggests the gas-phase structure at near room temperature is best described as an ensemble of *equatorial* and *axial* conformers [7], the IR/Raman study observed weak evidence for the axial form only in the gas-phase Raman spectrum. However, the IR study [6] also observed inhomogenous, temperature-dependent broadening in the equatorial absorptions, which they associate with structural averaging across a broad, shallow potential energy surface. The highest resolution study of this large amplitude motion is in femtosecond rotational coherence spectroscopy study of cyclopentane, by Kowalewski *et al.,* whom observed an energy level structure associated with the 10-fold symmetric pseudorotation potential of cyclopentane with an effective rotational constant of $B \approx 2.8\ cm^{-1}$ [10]. The presence of a SiH_3 / SiF_3 group in the molecules studied here breaks this

* Corresponding authors.
E-mail addresses: guirgisg@cofc.edu (G.A. Guirgis), nseifert@newhaven.edu (N.A. Seifert).

https://doi.org/10.1016/j.jms.2022.111698
Received 6 June 2022; Received in revised form 9 August 2022; Accepted 23 September 2022
Available online 17 October 2022

10-fold symmetry, so in the gas-phase one would expect two zeroth-order *equatorial* and *axial* conformers that may or may not be vibrationally perturbed by a large amplitude ring twisting mode.

Theoretical results show that the presence of a silicon substitutent lead to a significant stabilization of the *axial* substituted cyclopentane due to hyperconjugative effects. This can be interpreted as a 5-member equivalent of the anomeric effect found in substituted cyclohexanes, where electrostatic effects of polarized substitutents stabilize the axial form enough to negate the steric repulsion in the *axial* isomer. For instance, *axial* chlorocyclopentane is observed to be approximately 120–150 cm^{-1} more stable than the *equatorial* form [11,12], but bromocyclopentane prefers the *equatorial* form by approximately 93 ± 23 cm^{-1} [13]. However, methylcyclopentane is observed only in its *equatorial* form at room temperature [14–16]. Given the electronegativity difference between carbon and silicon, one would expect a silane-substituted cyclopentane will fall somewhere between the extremes of the halogen and methylated examples.

The use of broadband chirped-pulse Fourier transform microwave (CP-FTMW) spectroscopy and a molecular beam sample source is a natural continuation of these initial spectroscopic studies. While one is not guaranteed Boltzmann averaging of all minima in the puckering potential due to the inherently non-thermodynamic environment of the molecular beam, there is a virtual guarantee that observation of the global minimum along this surface is possible [17]. One may also be able to make some assessments on how large amplitude motion affects the zeroth order structure of CPS. Additionally, the fluorination of the silane group in TFCPS provides additional chemical complexity. Since the silicon-carbon bond is already significantly polarized due to poor valence overlap, the fluorination will only exacerbate the relative lack of covalent character, and we will use as impetus to explore the structural and dynamical differences between these two compounds.

2. Experimental and Theoretical methods

The syntheses of CPS and TFCPS were carried out at the College of Charleston, prepared in two steps. Cyclopentylbromide was reacted with magnesium in dry ether using the Grignard method and then coupled with tetrachlorosilane in dry ether under dry nitrogen gas. The resultant product cyclopentyltrichlorosilane was separated from the ether under reduced pressure and then reduced with lithium aluminum hydride in dry dibutyl ether under dry nitrogen. 1,1,1-trifluorocyclopentylsilane (TFCPS) was prepared by the fluorination of the trichloro derivative using freshly sublimed antimony trifluoride without solvent. Each sample was then purified by trap-to-trap distillation several times at reduced pressure and low temperature to isolate pure material. The isolated products were then verified by NMR spectroscopy. The NMR (400 MHz, $CDCl_3$) data for CPS is ^{1}H (δ (ppm)): 3.52 (d), 1.89(m), 1.56 (m), 1.55(m), 1.34(m), 1.14(m); ^{13}C NMR (400 MHz, $CDCl_3$): δ (ppm) 30.73, 27.03, 17.70; ^{29}Si (δ (ppm), 53.26. For TFCPS, the NMR assignments are: ^{1}H (δ (ppm)): 1.94 (m), 1.71(m), 1.62(m), 1.32(m); ^{13}C NMR (400 MHz, $CDCl_3$): δ (ppm) 26.88 (s), 26.35 (s), 17.72 (q); ^{29}Si (δ (ppm)), −59.67 (q).

The structure determination experiments using microwave spectroscopy were performed at Missouri S&T using a chirped-pulse Fourier transform microwave spectrometer, the design of which has been described in detail previously [18–20]. The spectral data was acquired using a traditional single-antenna detection arrangement for this instrument. Spectra were obtained using 4 μs chirps in three separate scans in the bands of 5.5–10.25 GHz, 9.75–14.5 GHz, and 14.0–18.75 GHz. Each scan was acquired by coherently averaging 3, 20 μs free induction decay signals per gas pulse from a supersonic expansion generated from a Parker-Hannifin Series 9 pulsed valve at a repetition rate of 3 Hz. In total, the spectra in the three aforementioned microwave bands were averaged in the time-domain from coherent averages of 108 200, 100 000 and 111 600 free induction decays, respectively. A Kaiser-Bessel window (β = 8.0) was then applied to these averaged time-domain signals before applying a Fourier transform to the frequency domain, in order to improve baseline resolution. The FWHM of the observed rotational transitions are approximately 120 kHz using this window function.

Experimental assignments and determination of rigid rotor parameters and centrifugal distortion constants for cyclopentylsilane and (trifluoro)-cyclopentylsilane were made by making an initial spectroscopic assignment using JB95, which was then refined using Kisiel's AABS software front-end [21] for Pickett's CALPGM rovibrational spectra fitting and prediction program suite [22,23]. Transition center frequencies were further refined by cubic interpolating the frequency domain spectra to a frequency spacing of 2 kHz, and then applying the Gaussian lineshape fitting routine in AABS to accurately determine the center frequencies. All species were fit using the I^r representation of the Watson S-reduced Hamiltonian.

All *ab initio* and density functional theory calculations were performed using Psi4. [24] All molecular structures presented here were roughly optimized using MP2/6–311++g(d,p) using the Psi4 driver of geomeTRIC optimization library [25] and then reoptimized at the B3LYP-D3/def2-TZVP level of theory with a very tight RMS displacement convergence criteria of 4.0×10^{-6} in order to ensure proper structural convergence in systems exhibiting a shallow potential energy surface. Vibrational calculations and potential energy scans were all performed at the MP2/6–311++g(d,p) level of theory using these B3LYP-D3 optimized structures.

3. Results

Like cyclohexane, cyclopentane exhibits a dynamical isomerization along a pseudorotational coordinate between equivalent structures. In cyclopentane, the minima along this 10-fold symmetric coordinate are called *bent* isomers and have formal C_s symmetry, with a planar D_{5h} geometry of acting as saddle-point interconnecting each *bent* isomer [9]. By adding a symmetric substituent like a silane group, the C_s symmetry of the frame should still be conserved, but now the hydrogens on each carbon are no longer chemically equivalent, which leads to the presence of two "envelope"-like conformers, *axial* and *equatorial*. Optimization of two guess *axial* and *equatorial* structures at the B3LYP-D3/def2-TZVP level of theory shows that both are in fact minima at equilibrium. The B3LYP-D3 predicted values of the rotational constants and dipole moments for these two conformers in both CPS and TFCPS can be found in Table 1, and a depiction of the two predicted conformers for each molecule can be found in Fig. 1.

Comparison of the predicted spectra to the experimental spectra led immediately to the assignment of the equatorial conformer of both molecules, which both show intense near-prolate *a*-type spectra. A visual overview of the CP-FTMW spectra of CPS and TFCPS can be found in Fig. 2. Initial assignment of the *a*-type spectra led to accurate enough rotational constants to detect a weaker set of *c*-type transitions and confirm a non-detection of *b*-type transitions, in agreement with the

Table 1
Predicted rotational constants, dipole component magnitudes, and equilibrium relative energies of TFCPS and CPS, calculated at the B3LYP-D3/def2-TZVP level of theory.

	B3LYP-D3/def2-TZVP			
	1,1,1-trifluorocyclopentylsilane		cyclopentylsilane	
	equatorial	axial	equatorial	axial
A / MHz	2529.2	2250.7	6008.6	4423.3
B	853.45	1022.9	1752.0	2101.0
C	776.05	955.5	1465.0	1891.1
$\lvert\mu_a\rvert$ / D	0.95	2.67	0.95	1.01
$\lvert\mu_b\rvert$ / D	0.00	0.00	0.00	0.00
$\lvert\mu_c\rvert$ / D	0.23	0.36	0.24	0.20
ΔE / cm^{-1}	0	411	0	508

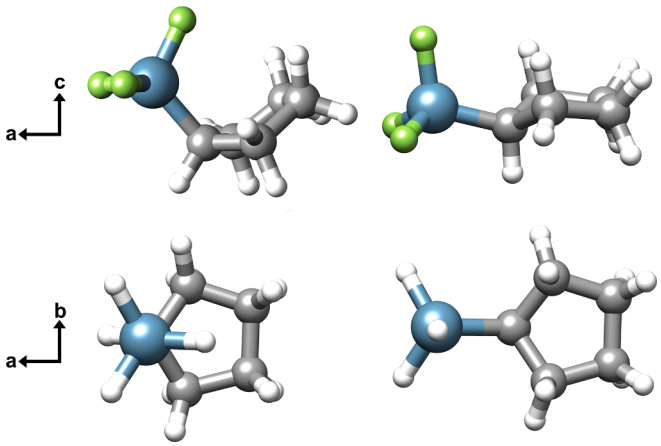

Fig. 1. B3LYP-D3/def2-TZVP predicted structures of axial (left) and equatorial (right) 1,1,1-trifluorocyclopentylsilane (TFCPS, top) and cyclopentylsilane (CPS, bottom). Since both molecular structures are similar, we show the TFCPS structures projected along the *ac*- inertial plane, and CPS along the *ab*- inertial plane.

prediction that CPS/TFCPS are C_s symmetric. The fitted spectroscopic constants for all species can be found in Table 2 and Table 3 for CPS and TFCPS, respectively, and the full line lists are available in the ***Supplementary Material***. In fact, the dynamic range afforded by the CP-FTMW experiment was sufficient enough to observe all possible singly-substituted heavy atom isotopologues of both molecules. The acquisition of singly-substituted isotopologue spectra enables direct structure determination of the heavy atom backbone of both the CPS and TFCPS molecules using Kraitchman's equations, the results of which can be found in Table 4 [26].

In the spectra of both molecules only one conformer was observed, consistent with the C_s-symmetric envelope conformation with an equatorial SiX_3 group. While the IR/Raman measurements of Durig and coworkers, [6] and the electron diffraction results from Shen & Dakkouri [7] suggest a dynamical equilibrium between the axial and equatorial forms of CPS, there are no such guarantees in a cold molecular beam environment. The B3LYP-D3/def2-TZVP relative energy between the axial and equatorial CPS is 508 cm^{-1}, in qualitative agreement with the 489 cm^{-1} energy difference presented in Durig. However, those older calculations also suggest a tiny interconversion barrier of 67 cm^{-1} from axial to equatorial. From a collisional point of view, interconversion from the axial to the equatorial form is almost certainly efficient, even with helium as the carrier gas. But given Durig's observation of a 70 cm^{-1} vibrational band in CPS, the 35 cm^{-1} zero point energy of this mode is almost certainly enough to generate considerable tunneling amplitude across this barrier [27]. Therefore, there is no empirical reason that the axial form would be observable in a molecular beam expansion.

No unidentified splittings or broadened lineshapes were observed in the parent or isotopic species, which indicate that internal rotation tunneling splittings from the SiH_3 and SiF_3 groups are not observable at the linewidths afforded by the CP-FTMW technique. However, this may not be particularly surprising when considering results of the internal rotation barriers of similar silanes. For instance, a study by Ocola and Laane on the internal rotation barriers of substituted cyclopropanes determine a reasonably high threefold barrier of $V_3 = 694$ cm^{-1} in cyclopropylsilane, which for a CH_3 group would generally lead to observable splittings in the microwave region [28]. However, the rotational constant for the SiH_3 rotor ($F = 3.378$ cm^{-1}) is significantly smaller than that of CH_3 ($F = 5.755$ cm^{-1}), so the torsional ground state is proportionally quite a bit deeper within the potential well than its CH_3 sibling. This would lead to smaller tunneling splittings between A and E components of the ground torsional state, leading to an almost certainly small splittings in the microwave region. Additionally, given the even more diminutive rotational constant for -SiF_3, it comes as no surprise that no splittings were observed in the TFCPS spectrum.

However, once the isotopic spectra were assigned and cut from the experimental spectrum, an unknown but clearly resolvable *a*-type

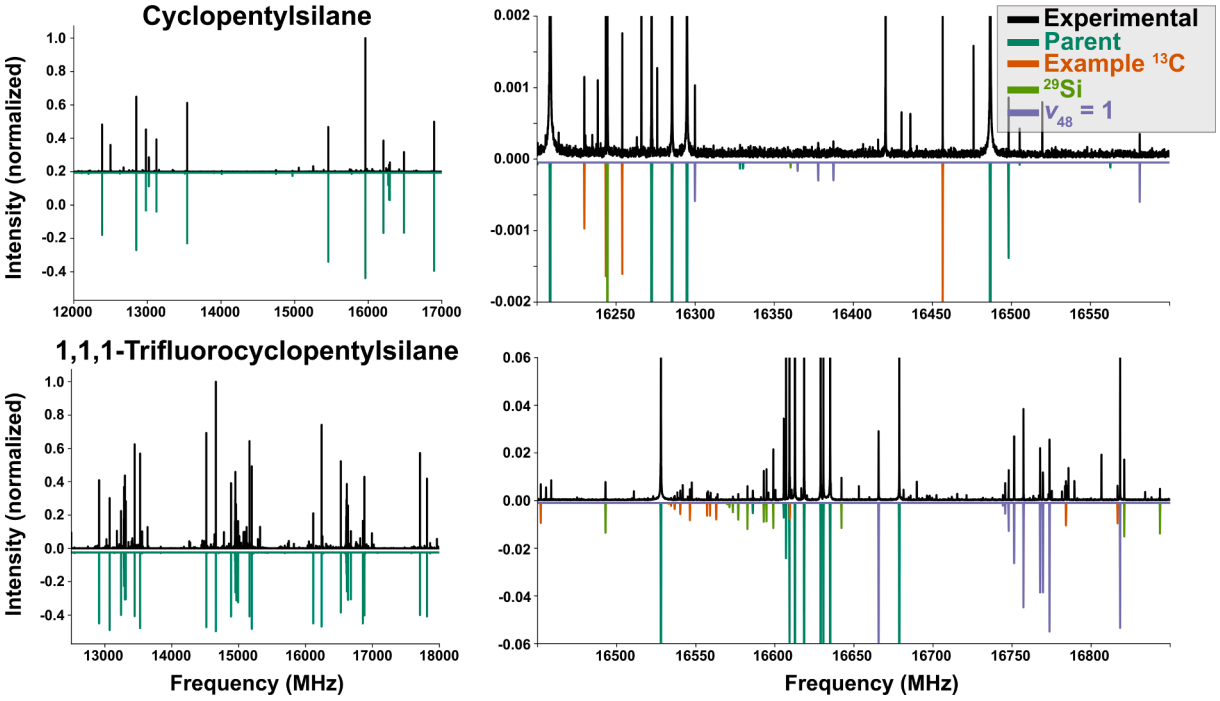

Fig. 2. Graphical overview of CPS and TFCPS broadband microwave spectra. Large bandwidth sections of CPS (top left) and TFCPS (bottom left) with predicted spectra of parent isotopic species are shown (negative valued spectra). In the right insets, zoomed views showing example isotopic and excited vibrational state spectra are shown for CPS (top right) and TFCPS (bottom right), along with uniquely colored predicted spectra of each species. Some intense transitions in the zoomed views have been vertically cut off to show detail.

Table 2
Fitted rotational constants for cyclopentylsilane, its observed isotopologues, and the observed spectrum associated with the $\nu_{48} = 1$ state of ring twisting vibrational mode.

	Parent	^{13}C(1)	^{13}C(2)	^{13}C(3)
A / MHz	5977.54789 (58)[A]	5936.432(19)	5877.409(48)	5965.784(66)
B	1768.83805 (21)	1745.08622 (53)	1767.17365 (49)	1767.31316 (63)
C	1479.26443 (18)	1460.21298 (50)	1472.02365 (46)	1478.96232 (59)
D_J / kHz	0.16666(98)	*[0.16666]*[B]	*[0.16666]*	*[0.16666]*
D_{JK}	0.4215(72)	*[0.4215]*	*[0.4215]*	*[0.4215]*
D_K	1.893(30)	*[1.893]*	*[1.893]*	*[1.893]*
d_1	−0.02147(22)	*[-0.02147]*	*[-0.02147]*	*[-0.02147]*
d_2	−0.00263(10)	*[-0.00263]*	*[-0.00263]*	*[-0.00263]*
N_{lines}[C]	118	31	29	25
ν_{rms} / kHz[D]	7.2	6.9	6.6	5.8
	^{29}Si	^{30}Si	$\nu_{48} = 1$	
A / MHz	5977.350(51)	5977.228(64)	5927.00(12)	
B	1742.01975 (21)	1716.56140 (57)	1777.8645 (12)	
C	1460.46936 (21)	1442.54021 (59)	1488.6241 (15)	
D_J / kHz	*[0.16666]*	*[0.16666]*	0.260(20)	
D_{JK}	*[0.4215]*	*[0.4215]*	−0.232(63)	
D_K	*[1.893]*	*[1.893]*	*[0]*	
d_1	*[-0.02147]*	*[-0.02147]*	*[0]*	
d_2	*[-0.00263]*	*[-0.00263]*	*[0]*	
N_{lines}	33	33	23	
ν_{rms} / kHz	7.6	7.2	10.2	

[A] Reported spectroscopic constant errors are 1σ adjusted standard errors assuming a frequency uncertainty of 25 kHz.
[B] Centrifugal distortion constants were fixed to the parent values for all isotopologues since they are not independently determinable at the typical sample size (N_{lines}) of observed transitions.
[C] N_{lines} is the number of assigned spectroscopic transitions.
[D] σ is the RMS error of the spectroscopic fit.

Table 3
Fitted rotational constants for 1,1,1-trifluorocyclopentylsilane, its observed isotopologues, and the observed spectrum associated with the $\nu_{48} = 1$ state of ring twisting vibrational mode.

	Parent	^{13}C(1)	^{13}C(2)	^{13}C(3)
A / MHz	2545.72209 (56)[A]	2537.577(11)	2527.132(45)	2542.742(51)
B	869.03506(19)	857.33327 (11)	866.01371 (38)	867.89703 (42)
C	790.60270(17)	780.32573 (11)	786.30353 (38)	789.95252 (42)
D_J / kHz	0.26446(61)	*[0.26446]*[B]	*[0.26446]*	*[0.26446]*
D_{JK}	−0.1536(24)	*[-0.1536]*	*[-0.1536]*	*[-0.1536]*
D_K	0.463(15)	*[0.463]*	*[0.463]*	*[0.463]*
d_1	−0.00711(32)	*[-0.00711]*	*[-0.00711]*	*[-0.00711]*
d_2	0.031049(85)	*[0.031049]*	*[0.031049]*	*[0.031049]*
N_{lines}[C]	217	68	64	65
ν_{rms} / kHz[D]	13.8	12.1	12.3	13.4
	^{29}Si	^{30}Si	$\nu_{48} = 1$	
A / MHz	2545.710(31)	2545.776(32)	2535.794(54)	
B	867.08447(25)	865.17158 (26)	876.00039 (73)	
C	788.98783(24)	787.40306 (26)	797.43309 (71)	
D_J / kHz	*[0.26446]*	*[0.26446]*	0.15995(99)	
D_{JK}	*[-0.1536]*	*[-0.1536]*	−0.1967(74)	
D_K	*[0.463]*	*[0.463]*	*[0]*	
d_1	*[-0.00711]*	*[-0.00711]*	−0.0065(17)	
d_2	*[0.031049]*	*[0.031049]*	−0.01233 (94)	
N_{lines}	83	81	85	
ν_{rms} / kHz	8.7	8.7	8.3	

[A] Reported errors on spectroscopic constants are 1σ adjusted standard errors, assuming a frequency uncertainty of 25 kHz.
[B] Centrifugal distortion constants were fixed to the parent values for all isotopologues since they are not independently determinable at the typical sample size (N_{lines}) of observed transitions.
[C] N_{lines} is the number of assigned spectroscopic transitions.
[D] ν_{rms} is the RMS error of the spectroscopic fit.

spectrum was present in the spectra of both CPS and TFCPS. Upon assignment, these unknown spectra exhibit rotational constants and observed relative intensities that are quite similar to that of the parent isotopic species, suggesting structural similarity. However, the experimental values for the rotational constants B and C are both larger than the values observed in the parent isotopic species, indicative of a slight expansion of the structure along its near-prolate symmetry axis. This expansion suggests that this unknown spectrum is one of an excited vibrational state of the molecule. However, the fit also suggests no additional non-rigidity in this unknown state, e.g. from anomalously large centrifugal distortion constants or a poor statistical fit, compared to the parent species. These observations are tell-tale signs that this state is associated with an excited vibrational state or tunneling component of a symmetric motion corresponding to a pseudorotational, low-lying twisting mode of the cyclopentane ring, or at least some low-lying state that has no observable rovibrational coupling to the ground vibrational state.

In the CPS spectrum, the intensity of this excited state spectrum is quite weak, even weaker than the ^{13}C spectra (ca. 0.1 % of parent intensity). However, in the TFCPS spectrum, the relative intensity of this satellite spectrum is significantly more intense, nearly 25 % of the intensity of the parent species. This intensity variation between the two molecules clearly discounts that this excited state is part of a tunneling-derived pair of vibrational states that contains the parent isotopic spectrum as its other member, since such a motion would suggest a fixed intensity ratio from spin statistics. Rather, it may be a separate, low-lying vibrational state that is only partially cooled during the supersonic expansion, which would explain its weak intensity and the variance in the intensity between both molecules.

4. Discussion

4.1. Structure

The observed isotopic species suggest that both structures are C_s symmetric, as only 3 distinct ^{13}C spectra were observed for each, and two had approximately double intensity of the other due to chemical equivalence. Thus, these ^{13}C spectra correspond to the 1, 2-/5-, and 3-/4- positions on the cyclopentane ring. However, even in the r_s Kraitchman structures, which reflects some ground-state structural averaging, the cyclopentane ring appears to be puckered in its ground state form in the so-called "envelope" conformation, with a large negative inertial defect of $\Delta \approx -28.6$ amu Å^2 and a non-zero out-of-plane planar moment $P_{cc} \approx 14.3$ amu Å^2 for CPS.

In comparison to cyclopentane, where the C—C bond lengths range from 1.528 to 1.552 Å in the bent isomer, we observe similar, Kraitchman determined, C—C bond lengths in cyclopentylsilane, ranging from 1.527(18) Å for the ^{1}C–^{2}C bond to 1.5502(39) Å for the ^{3}C–^{4}C bond, consistent with the alternating bond length trends in standard cyclopentane [10], as shown in Table 4. This suggests the SiH_3 substituent contributes very little bond length perturbation to the ring backbone. However, the Kraitchman puckering dihedral of the ^{1}C atom is significantly different than in cyclopentane, which is 41.5° in cyclopentane and 32.6(15)° in CPS. This is even in disagreement with the calculated B3LYP-D3 equilibrium structure of CPS, which has a puckering angle of approximately 24.6°. This seems to be general amongst both CPS and TFCPS, where the ^{3}C–^{4}C r_s positions are slightly skewed out of the ring plane with respect to the equilibrium structure. In CPS, this effect seems more pronounced in the ^{1}C and ^{5}C coordinates, but to a lesser extent

Table 4
Derived heavy atom structural parameters from experiment using Kraitchman's equations [r_s], least squares determination [$r_m^{(1)}$] and B3LYP-D3/def2-TZVP calculations. The B3LYP-D3 structures are optimized to a C_s symmetric minimum, and the $r_m^{(1)}$ structure is calculated using the same symmetry constraint.

	cyclopentylsilane			1,1,1-trifluorocyclopentylsilane		
Bond Lengths / Å	r_s	$r_m^{(1)}$	B3LYP-D3	r_s	$r_m^{(1)}$	B3LYP-D3
r[^{1}C- Si]	1.8914(94)	1.8855(93)	1.8819	1.931(15)	1.918(48)	1.8391
r[^{1}C - ^{2}C]	1.527(18)	1.5241(66)	1.5412	1.482(36)	1.481(84)	1.5448
r[^{2}C - ^{3}C]	1.5457(41)	1.5543(40)	1.5444	1.4820(64)	1.446(35)	1.6678
r[^{3}C - ^{4}C]	1.5502(39)	1.5535(28)	1.5535	1.5123(29)	1.507(37)	1.5528
r[^{4}C - ^{5}C]	1.5457(41)	1.5543(40)	1.5444	1.4828(84)	1.448(35)	1.6678
r[^{5}C - ^{1}C]	1.527(18)	1.5241(66)	1.5412	1.482(36)	1.481(84)	1.5448
Bond Angles / °						
∠[Si - ^{1}C –^{2}C]	118.5(22)	113.79(36)	115.07	111.6(27)	111.9(40)	114.88
∠[^{1}C - ^{2}C - ^{3}C]	107.89(53)	103.93(45)	104.53	97.0(12)	99.9(52)	96.82
∠[^{2}C - ^{3}C - ^{4}C]	105.00(26)	105.63(14)	105.87	108.03(16)	108.0(19)	104.85
∠[^{3}C - ^{4}C- ^{5}C]	105.00(26)	105.63(14)	105.87	108.03(16)	108.0(19)	104.85
∠[^{4}C - ^{5}C - ^{1}C]	107.89(53)	103.93(45)	104.53	97.0(12)	99.9(52)	96.82
∠[^{5}C -^{1}C - Si]	113.48(21)	113.79(36)	115.07	112.8(26)	111.9(40)	114.88
Bond Dihedrals / °						
τ[Si - ^{1}C - ^{2}C - ^{3}C]	−151.8(15)	−164.32(67)	−164.98	−170.3(24)	−160.8(89)	−178.86
τ[^{1}C - ^{2}C - ^{3}C - ^{4}C]	0.2(14)	0.0(11)	0.0	0.0(24)	0.0(19)	0.0
τ[^{2}C - ^{3}C -^{4}C - ^{5}C]	20.5(15)	24.7(11)	24.58	24.7(18)	22.7(16)	32.47
τ[^{3}C - ^{4}C - ^{5}C - ^{1}C]	−20.5(13)	−24.7(11)	−24.58	−24.7(18)	−22.7(16)	−32.47
τ[^{4}C -^{5}C - ^{1}C - Si]	167.0(17)	164.32(67)	164.98	169.3(28)	162.8(89)	178.86

than in TFCPS.

An instructive and recent example of this failure of Kraitchman's equations is in the rotational spectra of partially fluorinated cyclopentanes, reported by Minei and Cooke [29]. The authors observe non-physical carbon–carbon bond lengths in these cyclopentanes as determined by Kraitchman's equations, due to appreciable dependence on isotopic substitution in the overall vibrational averaging of the structure, which leads to appreciable differences between the ground state structures of the parent and its corresponding isotopologues. These discrepancies violate the primary assumption in Kraitchman's equations, which is that the vibrationally averaged structure of the molecule does not appreciably change upon heavy atom isotopic substitution.

However, this deviation between the B3LYP-D3 and Kraitchman structures can partially be rationalized by noting that a number of Cartesian coordinates for the ring carbons, tabulated in Tables S5 and S6 in the Supplementary Material, are imaginary due to their values being close to an inertial axis, a well-known limitation of the Kraitchman equations. In order to compensate for these discrepancies, we applied the $r_m^{(1)}$ least-squares method of Watson, Roytburg and Ulrich, to determine a more reasonable experimental structure [30]. In this determination, a C_s symmetric structure was assumed, the SiH_3 / SiF_3 groups were fixed to a staggered configuration, and that the total sum of the dihedrals of the hydrogen and fluorine substituents sum to zero. This was important in the case of the SiF_3 analogue, since the lack of fluorine isotopic information, combined with the trifluorosilane group's large contribution to the total moment of inertia of the molecule, leads to poor convergence if these structural assumptions are at all relaxed. However, even with these assumptions, the statistical certainty of the SiF_3 analogue is overall worse than SiH_3, with a χ^2 value of ca. 0.05 compared to the SiH_3 χ^2 of 0.00037 (# DOF = 10 for both species).

Thankfully, the $r_m^{(1)}$ determination, tabulated in Table 4, mitigates the near-axis uncertainties in the Kraitchman structures, although both are in qualitative agreement each other. A figure comparing the B3LYP-D3 structures of CPS and TFCPS to the Kraitchman coordinates can be found in Fig. 3. The difference between the B3LYP-D3 equilibrium and two experimental ground-state structures of CPS are quite similar; however, there is a significant discrepancy between the equilibrium and the vibrationally averaged ground state structure of TFCPS. In TFCPS, both Kraitchman and $r_m^{(1)}$ show significant lengthening of the C-Si bond relative to the B3LYP-D3 value, and shortening of the C—C bonds. Similar behavior can be seen in the angular and dihedral parameters, as well. However, given the analysis presented later in this study on the lowest-lying ring puckering vibrational mode, TFCPS is significantly more anharmonic near the equilibrium structure. Therefore, the experimental ground state structure, whose structural parameters are proportional to the expectation value $\langle 1/r^2 \rangle^{-\frac{1}{2}}$, will be necessarily different than those calculated at equilibrium for such an anharmonic potential.

In TFCPS the fluorines clearly contribute more significantly to the structural perturbation of the ring. The C—C bonds in TFCPS exhibit similar trends but are quite a bit shorter than those in CPS, ranging from 1.446(35) to 1.507(37) Å. The puckering dihedral angle difference between equilibrium and ground state also switches signs relative to CPS,

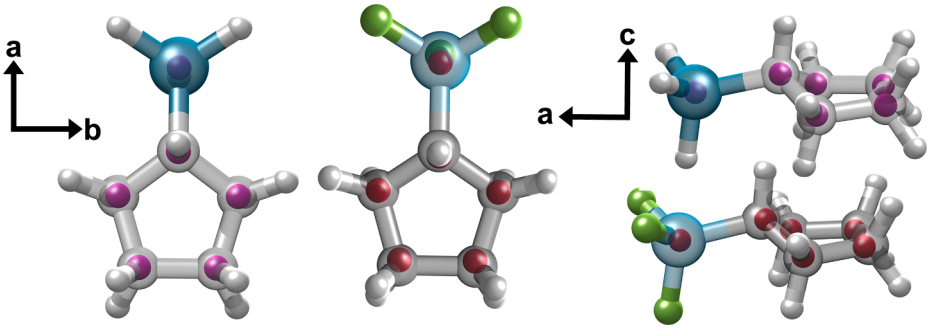

Fig. 3. Top and side comparisons of B3LYP-D3/def2-TZVP structures (large ball & stick models) to the experimental $r_m^{(1)}$ structure (small pink spheres) for cyclopentylsilane (left; top right) and 1,1,1-trifluorocyclopentylsilane (right, bottom right). 2D projections of the inertial axis system for each view are also shown. (For interpretation of the references to colour in this figure legend, the reader is referred to the web version of this article.)

perhaps coincidentally; we measure 22.7(16)° in the $r_m^{(1)}$ structure, and the B3LYP-D3 equilibrium value is 32.5°! Electronically, these differences are perhaps not so surprising; silicon is less electronegative than carbon, so we expect the carbon backbone to have a slightly negative electrical polarization. The fluorines only exacerbate this electronegative difference, by polarizing what little valence electron density in the silicon further away from Si-C bond, which should only serve to strengthen the C—C bonds in the ring.

4.2. Excited vibrational states

In order to identify the vibrational carrier of the "excited state" spectrum observed for both TFCPS and CPS, we apply a simple but effective heuristic argument using basic perturbation theory in order to make some useful conclusions about the vibrational mode associated with these spectra.

Both TFCPS and CPS exhibit primarily *a*-type spectra and have near-prolate Ray's asymmetry parameters: −0.87 and −0.91, respectively. Therefore, we can roughly approximate any rovibrational effects by assuming a symmetric top-like, $\Delta K = 0$, rotational spectrum associated with a single rotational constant B_0, which we approximate here as $B_0 \approx \frac{1}{2}(B+C)$. In this approximation, the rovibrational energy of a rigid rotor state is $E(v,J) = B_v J(J+1) = [B_e - \alpha_e(v+\frac{1}{2})]J(J+1)$, where α_e is the vibration-rotational interaction constant for a given vibrational state. Since we only observe a lone vibrationally excited spectrum, we need only consider the value of a single α_e coefficient.

The vibrational potential energy is then expanded along this normal mode coordinate as a Taylor series:

$$V(\boldsymbol{Q}) = \frac{1}{2}k\boldsymbol{Q}^2 + \frac{1}{6}a\boldsymbol{Q}^3 + \frac{1}{24}b\boldsymbol{Q}^4 + O(\boldsymbol{Q}^5)$$

Applying perturbation theory, the harmonic correction to the rotational energy upon vibrational excitation is $\alpha_e^{(1)} = -6B_e^2/\omega_e$ where $\omega_e = \left(\frac{k}{\mu}\right)^{\frac{1}{2}}$ is the harmonic frequency of the vibrational mode. The leading order anharmonic correction, proportional to $O(\mathbf{Q}^3)$, is:

$$\alpha_e^{(2)} = -4a\left[\frac{\hbar}{2c\mu\omega_e}\right]^{\frac{3}{2}}$$

Substituting $B_e \approx \frac{1}{2}(B_0 + C_0)$, the total vibrational correction to the rotational constant to order $O(Q^3)$ is:

$$\alpha_e = \alpha_e^{(1)} + \alpha_e^{(2)} = -\frac{3(B_0+C_0)^2}{\omega_e} - 4a\left[\frac{\hbar}{2c\mu\omega_e}\right]^{\frac{3}{2}}$$

Since the only unknown parameters here are *a*, the cubic coefficient of the potential, the harmonic frequency ω_e and the reduced mass of the motion μ, we can easily estimate the value of α_e by calculating the harmonic frequencies of the molecule and the potential $V(\mathbf{Q})$ for the chosen vibrational mode using electronic structure theory. Experimentally, we can measure a value of this approximate α_e by measuring the change in $\frac{1}{2}(B+C)$ between the ground and excited state spectra. For instance, a red-shift between the $\nu = 0$ and $\nu = 1$ spectra imply a negative value for α_e, as observed in the experimental spectrum.

The question remains: what vibrational mode is the most likely carrier of this unidentified rotational spectrum? Given the molecular beam environment and its highly efficient vibrational cooling, the most likely candidate would be the lowest lying normal mode of either molecule, which is the so-called ring twisting normal mode, ν_{48}, of these molecules. Fig. 4 shows a simplified diagram of the out-of-plane motion associated with this twisting mode. This mode is a member of the A'' irreducible representation of the C_s point group, which leads to an anti-symmetric motion anti-symmetric about the prolate symmetry axis.

An MP2/6–311++g(d,p) frequency calculation using Psi4 results in $(\omega_e, \mu) = (31\text{cm}^{-1}, 1.5551\text{amu})$ and $(16\text{cm}^{-1}, 1.7827\text{amu})$ for CPS and TFCPS, respectively. One could certainly apply VPT2 methods [31] to calculate the anharmonic corrections to this mode, but we have decided to use a slightly different approach to make estimates for the physical observable we can observe in our rotational spectrum, which is the value of α_e.

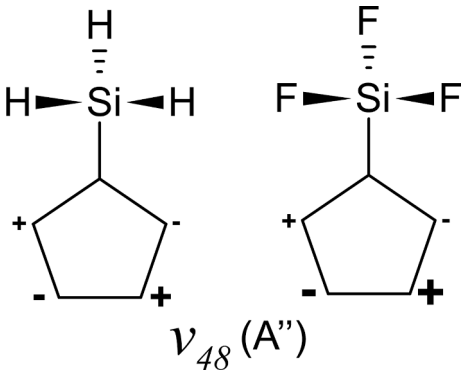

Fig. 4. Simplified diagram of the ν_{48} normal mode of CPS and TFCPS the out-of-plane anti-symmetric displacement of the ring carbons, assuming a C_s symmetry. + labeling implies displacement above the *ab*-inertial plane, and – labeling implies displacement below the plane.

In order to calculate the potential energy surface along this normal mode, we distort the molecule along a trajectory parallel to the v_{48} normal mode eigenvector using small Cartesian displacements from the minimum structure. These displacements are in units of Angstroms, but are normalized such that the eigenvector of the normal mode has a magnitude of unity. This allows us to use the reduced masses from the frequency calculation, which are calculated assuming the magnitude of the normal mode eigenvectors are normalized to unity. In order to make a direct comparison between the CPS and TFCPS potentials, we also convert the Cartesian displacements to mass-weighted displacements in the typical way, e.g. for the j^{th} atom, $\Delta x_j' = \Delta x_j \sqrt{m_j}$.

Once the potential $V(x)$ was calculated for both CPS and TFCPS at the MP2/6–311++g(d,p) level of theory, we fit the region of the potential near the equatorial conformers using a 3rd order polynomial, potential $V(x) = \frac{1}{6}ax^3 + \frac{1}{2}kx^2$; since we are only concerned with the v = 0 and v = 1 states of this mode, we need not fit the entire potential to a function; a local Taylor expansion is sufficient. For CPS, the potential fit gives values of $k = 41.78(27)$ and $a = -3.1(27)x10^{-8}$; for TFCPS, these coefficients are $k = 26.413(66)$ and $a = 2.97(43)x10^{-8}$. Note that these potentials are not appreciably anharmonic within 100 cm^{-1} of the minimum. A plot of the potentials near the equatorial minima for both molecules and their first few eigenstates can be found in Fig. 5.

In order to calculate the vibrational states associated with these potentials, we must assume some effective mass for the motion and then and numerically solve the Schrodinger equation using the discrete variable representation. This leads to predicted frequencies of $\omega_e = 30\text{cm}^{-1}$ and 16cm^{-1} for CPS and TFCPS, respectively. These frequencies are much lower than the low-frequency mode assigned with the observations of Durig and coworkers, who assign the CPS ring twisting mode ν_{48}, to a 70 cm^{-1} component observed in a Raman combination band of the SiH_3 stretching mode [6].

With these potentials and eigenvalues in hand, estimations can be made for the values of α_e for both species. The calculated values for α_e from this potential fit are −16.5 MHz and −8.7 MHz for CPS and TFCPS respectively. These values show a similar reduction of α_e from CPS to TFCPS as the experimental values of −9.19 MHz and −6.90 MHz reflect, but are not in quantitative agreement. However, if we consider that the curvature near the minimum of these potential energy surfaces are inaccurate due to the level of theory applied, we can appeal to the observed Raman assignment of ν_{48} at approximately 70 cm^{-1} [6] Assuming $\omega_{e,CPS} \approx 70cm^{-1}$ and that the ratio $\omega_e[TFCPS]/\omega_e[CPS] = 31/$

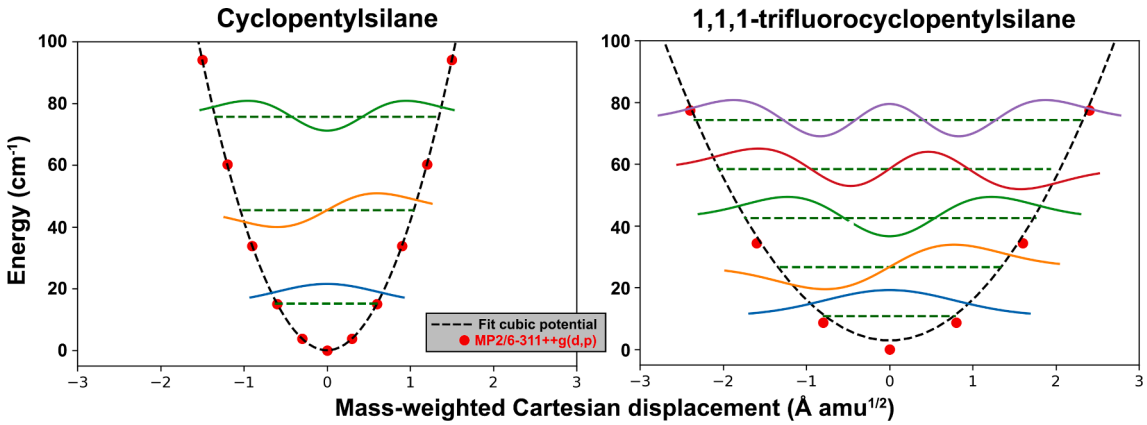

Fig. 5. Plots of the fitted cubic potential along the ν_{48} normal mode near the global minimum equatorial conformer of cyclopentylsilane and 1,1,1-trifluorocyclopentylsilane along their mass-weighted Cartesian displacements. The displacements are determined using the displacement eigenvector output from the normal mode calculation, then mass-weighted to place both species on the same displacement scale. *Ab initio* energies for this potential were calculated at the MP2/6–311++g(d,p) level of theory.

15 as predicted, the calculated α_e values would be −7.5 MHz and −4.6 MHz for CPS and TFCPS, which are much more consistent with the observed spectra.

The flattening of the equatorial potential for TFCPS is consistent with previous studies of similar molecules, such as halogenated 1-silacyclopent-2-enes, which exhibit similar flattening of their potential upon substitution of electronegative atoms such as fluorines [32,33]. Other substituted organosilicon ring structures, such as silacyclobutane, exhibit much lower fundamental frequencies for large amplitude modes upon fluorine substitution [34].

Our values for α_e are quite similar to those measured experimentally for the cyclopentane ring twisting mode. Kowalewski *et al.*'s femtosecond Raman rotational coherence spectroscopy measurements determined an α_e = -9.547(1) MHz for the ν_{23} mode of cyclopentane, equivalent to the ring twisting mode to that explored in CPS and TFCPS. The true lowest-lying state for cyclopentane, which is the 10-fold symmetric pseudorotational mode, has a diminutive $\alpha_e = 0.70(1)$ kHz, which helps to bolster an assignment of the observed excited state in the CPS and TFCPS spectra as a *bona fide* ring twisting mode [10]. Therefore, we are quite confident in our assignment that the observed vibrationally excited state in CPS and TFCPS is associated with this low-lying, large amplitude ring twisting mode.

5. Conclusions

In this study, we have presented the broadband microwave spectroscopy of two undergraduate-synthesized organosilicon molecules: cyclopentylsilane and 1,1,1-trifluorocyclopentylsilane. The microwave spectroscopy of these two molecules afforded excellent dynamic range, enabling structural determination of the heavy atom backbone of each molecule using natural isotopic substitution. Both molecules exhibit large amplitude motional effects due to the pseudorotational/puckering motion of the cyclopentane rings, arising from a shallow and anharmonic potential energy surface along this mode. This motion leads to both observable ground state structural effects, as well as incomplete vibrational cooling in the molecular beam environment. This incomplete cooling leads to a populated excited vibrational state, which we identify as the v = 1 state of the lowest lying ring twisting mode of the molecule through application of simple rovibrational perturbation theory.

This study is yet another interesting example of the positive feedback loop between synthetic chemists and spectroscopists; while most organic synthesis studies use traditional condensed-phase spectroscopic techniques for structure determination, the use of broadband microwave spectroscopy is an ideal method for those chemists who are interested in deeply understanding the structures of their synthesized molecules. The sensitivity afforded by broadband techniques enables careful study of the structure and potential energy surface of molecules, and the coupling to molecular beam techniques allows one to decouple structural isomerization routes that may be obscured by dynamical motional averaging in condensed phase or room temperature methods, such as the isomerization between axial and equatorial forms in the molecules studied here. Additionally, broadband microwave spectroscopy allows for significantly faster turnaround times between synthesis and structural assignment than previous microwave techniques, so we hope that organic chemists continue to exploit the obvious advantages of microwave techniques for their structural studies in the future.

CRediT authorship contribution statement

Lucas Licaj: Methodology. **Nicole Moon:** Investigation. **Garry S. Grubbs II:** Funding acquisition, Supervision, Writing – review & editing. **Gamil A. Guirgis:** Conceptualization, Project administration, Resources. **Nathan A. Seifert:** Formal analysis, Writing – original draft, Visualization.

Declaration of Competing Interest

The authors declare that they have no known competing financial interests or personal relationships that could have appeared to influence the work reported in this paper.

Data availability

Data will be made available on request.

Acknowledgements

This material is based upon work supported by the National Science Foundation under Grant no. CHE-MRI-2019072. GAG acknowledges the College of Charleston Faculty Research and Development Grant program; GAG and LL also acknowledge for The Major-Academic-year Support (MAYS) Program for the support of this research. GAG would also like to dedicate this paper to Prof. James P. Deavor, on the occasion of his retirement as Chair of the Chemistry and Biochemistry Department at the College of Charleston, and for all his essential help over the last 20 years. Finally, NAS acknowledges start-up and research funding from the Tagliatela College of Engineering at the University of New Haven.

Appendix A. Supplementary data

Supplementary data to this article can be found online at https://doi.org/10.1016/j.jms.2022.111698.

References

[1] H.V.L. Nguyen, W. Caminati, J.-U. Grabow, The LAM of the Rings: Large Amplitude Motions in Aromatic Molecules Studied by Microwave Spectroscopy, Molecules 27 (2022) 3948, https://doi.org/10.3390/molecules27123948.

[2] L. Xu, G.T. Fraser, F.J. Lovas, R.D. Suenram, C.W. Gillies, H.E. Warner, J.Z. Gillies, The microwave spectrum and OH internal rotation dynamics of gauche-2,2,2-trifluoroethanol, J. Chem. Phys. 103 (1995) 9541–9548, https://doi.org/10.1063/1.469968.

[3] J. van Wijngaarden, Z. Chen, C.W. van Dijk, J.L. Sorensen, Pure Rotational Spectrum and Ring Inversion Tunnelling of Silacyclobutane, J. Phys. Chem. A. 115 (2011) 8650–8655, https://doi.org/10.1021/jp205006v.

[4] J. Laane, Spectroscopic determination of ground and excited state vibrational potential energy surfaces, Int. Rev. Phys. Chem. 18 (1999) 301–341, https://doi.org/10.1080/014423599229974.

[5] G.G. Engerholm, A.C. Luntz, W.D. Gwinn, D.O. Harris, Ring Puckering in Five-Membered Rings. II. The Microwave Spectrum, Dipole Moment, and Barrier to Pseudorotation in Tetrahydrofuran, J. Chem. Phys. 50 (1969) 2446–2457. https://doi.org/10.1063/1.1671401.

[6] J.R. Durig, W. Zhao, X. Zhu, T.J. Geyer, M. Dakkouri, Spectra and structure of small ring compounds. LXV. Raman and infrared spectra, conformational stability, and vibrational assignment of cyclopentylsilane, J. Mol. Struct. 351 (1995) 31–49, https://doi.org/10.1016/0022-2860(94)08484-Y.

[7] Q. Shen, M. Dakkouri, The molecular structure and pseudorotational motion of cyclopentylsilane as determined by electron diffraction, J. Mol. Struct. 131 (1985) 327–332, https://doi.org/10.1016/0022-2860(85)87034-4.

[8] G. Wang, D. Li, E.C. Chelius, J.B. Lambert, Ab initio study of positive charge stabilization by silicon in five-membered rings, J. Chem. Soc., Perkin Trans. 2 (1990) 331–334, https://doi.org/10.1039/P29900000331.

[9] E.J. Ocola, L.E. Bauman, J. Laane, Vibrational spectra and structure of cyclopentane and its isotopomers, J. Phys. Chem. A. 115 (2011) 6531–6542, https://doi.org/10.1021/jp2032934.

[10] P. Kowalewski, H.-M. Frey, D. Infanger, S. Leutwyler, Probing the Structure, Pseudorotation, and Radial Vibrations of Cyclopentane by Femtosecond Rotational Raman Coherence Spectroscopy, J. Phys. Chem. A. 119 (2015) 11215–11225, https://doi.org/10.1021/acs.jpca.5b07930.

[11] R.C. Loyd, S.N. Mathur, M.D. Harmony, Microwave spectrum, conformation, and quadrupole coupling constants of cyclopentyl chloride, J. Mol. Spectrosc. 72 (1978) 359–371, https://doi.org/10.1016/0022-2852(78)90136-4.

[12] P. Groner, M.J. Lee, J.R. Durig, The microwave spectrum of the equatorial conformer of chlorocyclopentane, J. Chem. Phys. 94 (1991) 3315–3321, https://doi.org/10.1063/1.459754.

[13] J.R. Durig, W. Zhao, X. Zhu, Microwave spectrum, ab initio calculations, and structural parameters of bromocyclopentane, J. Mol. Struct. 521 (2000) 25–35, https://doi.org/10.1016/S0022-2860(99)00423-8.

[14] J.R. Durig, K.L. Kizer, J.M. Karriker, Spectra and structure of small ring compounds. XXXVI. 2-methyl-1,3-dioxolane; 2-methyl-1,3-dioxolane-d4; 2-methyltetrahydrofuran; and methylcyclopentane, J. Raman Spectrosc. 1 (1) (1973) 17–45.

[15] R.L. Lipnick, NMR spectroscopy of cyclopentane derivatives. III. Methylcyclopentane, J. Am. Chem. Soc. 96 (1974) 2941–2948, https://doi.org/10.1021/ja00816a046.

[16] V. Van, W. Stahl, M. Schwell, H.V.L. Nguyen, Gas-phase conformations of 2-methyl-1,3-dithiolane investigated by microwave spectroscopy, J. Mol. Struct. 1156 (2018) 348–352, https://doi.org/10.1016/j.molstruc.2017.11.084.

[17] F. Xie, X. Ng, N.A. Seifert, J. Thomas, W. Jäger, Y. Xu, Rotational spectroscopy of chiral tetrahydro-2-furoic acid: Conformational landscape, conversion, and abundances, J. Chem. Phys. 149 (22) (2018) 224306.

[18] F.E. Marshall, D.J. Gillcrist, T.D. Persinger, S. Jaeger, C.C. Hurley, N.E. Shreve, N. Moon, G.S. Grubbs, The CP-FTMW spectrum of bromoperfluoroacetone, J. Mol. Spectrosc. 328 (2016) 59–66, https://doi.org/10.1016/j.jms.2016.07.014.

[19] G. Sedo, F.E. Marshall, G.S. Grubbs, Rotational spectra of the low energy conformers observed in the (1R)-(−)-myrtenol monomer, J. Mol. Spectrosc. 356 (2019) 32–36, https://doi.org/10.1016/j.jms.2018.12.005.

[20] A. Duerden, F.E. Marshall, N. Moon, C. Swanson, K.M. Donnell, G.S. Grubbs II, A chirped pulse Fourier transform microwave spectrometer with multi-antenna detection, J. Mol. Spectrosc. 376 (2021), 111396, https://doi.org/10.1016/j.jms.2020.111396.

[21] Z. Kisiel, L. Pszczółkowski, I.R. Medvedev, M. Winnewisser, F.C. De Lucia, E. Herbst, Rotational spectrum of trans–trans diethyl ether in the ground and three excited vibrational states, J. Mol. Spectrosc. 233 (2005) 231–243, https://doi.org/10.1016/j.jms.2005.07.006.

[22] H.M. Pickett, The fitting and prediction of vibration-rotation spectra with spin interactions, J. Mol. Spectrosc. 148 (1991) 371–377, https://doi.org/10.1016/0022-2852(91)90393-O.

[23] S.E. Novick, A beginner's guide to Pickett's spcat/spfit, J. Mol. Spectrosc. 329 (2016) 1–7, https://doi.org/10.1016/j.jms.2016.08.015.

[24] J.M. Turney, A.C. Simmonett, R.M. Parrish, E.G. Hohenstein, F.A. Evangelista, J. T. Fermann, B.J. Mintz, L.A. Burns, J.J. Wilke, M.L. Abrams, N.J. Russ, M. L. Leininger, C.L. Janssen, E.T. Seidl, W.D. Allen, H.F. Schaefer, R.A. King, E. F. Valeev, C.D. Sherrill, T.D. Crawford, Psi4: an open-source ab initio electronic structure program, WIREs Comput. Mol. Sci. 2 (2012) 556–565, https://doi.org/10.1002/wcms.93.

[25] L.-P. Wang, C. Song, Geometry optimization made simple with translation and rotation coordinates, J. Chem. Phys. 144 (21) (2016) 214108.

[26] J. Kraitchman, Determination of Molecular Structure from Microwave Spectroscopic Data, Am. J. Phys. 21 (1953) 17–24, https://doi.org/10.1119/1.1933338.

[27] R.S. Ruoff, T.D. Klots, T. Emilsson, H.S. Gutowsky, Relaxation of conformers and isomers in seeded supersonic jets of inert gases, J. Chem. Phys. 93 (1990) 3142–3150, https://doi.org/10.1063/1.458848.

[28] E.J. Ocola, J. Laane, Internal Rotation of Methylcyclopropane and Related Molecules: Comparison of Experiment and Theory, J. Phys. Chem. A. 120 (2016) 7269–7278, https://doi.org/10.1021/acs.jpca.6b06783.

[29] A.J. Minei, S.A. Cooke, Evaluation of the substitution structures of two partially fluorinated cyclopentanes C5H3F7 and C5H2F8, J. Mol. Struct. 1207 (2020), 127778, https://doi.org/10.1016/j.molstruc.2020.127778.

[30] J.K.G. Watson, A. Roytburg, W. Ulrich, Least-Squares Mass-Dependence Molecular Structures, J. Mol. Spectrosc. 196 (1999) 102–119, https://doi.org/10.1006/jmsp.1999.7843.

[31] P.R. Franke, J.F. Stanton, G.E. Douberly, How to VPT2: Accurate and Intuitive Simulations of CH Stretching Infrared Spectra Using VPT2+K with Large Effective Hamiltonian Resonance Treatments, J. Phys. Chem. A. 125 (2021) 1301–1324, https://doi.org/10.1021/acs.jpca.0c09526.

[32] T.M.C. McFadden, N. Moon, F.E. Marshall, A.J. Duerden, E.J. Ocola, J. Laane, G. A. Guirgis, G.S. Grubbs, The molecular structure and curious motions in 1,1-difluorosilacyclopent-3-ene and silacyclopent-3-ene as determined by microwave spectroscopy and quantum chemical calculations, Phys. Chem. Chem. Phys. 24 (2022) 2454–2464, https://doi.org/10.1039/D1CP04286F.

[33] T.M.C. McFadden, F.E. Marshall, E.J. Ocola, J. Laane, G.A. Guirgis, G.S. Grubbs, Theoretical Calculations, Microwave Spectroscopy, and Ring-Puckering Vibrations of 1,1-Dihalosilacyclopent-2-enes, J. Phys. Chem. A 124 (40) (2020) 8254–8262.

[34] A.A. Al-Saadi, J. Laane, Structure, Vibrational Spectra, and DFT and ab Initio Calculations of Silacyclobutanes, Organometallics. 27 (2008) 3435–3443, https://doi.org/10.1021/om800296w.